IOP Publishing Journal of Physics D: Applied Physics
J. Phys. D: Appl. Phys. **49** (2016) 265602 (8pp) doi:10.1088/0022-3727/49/26/265602

Optical rectenna operation: where Maxwell meets Einstein

Saumil Joshi and Garret Moddel

Department of Electrical, Computer, and Energy Engineering, University of Colorado, Boulder, CO 80309-0425, USA

E-mail: moddel@colorado.edu

Received 1 February 2016, revised 8 April 2016
Accepted for publication 29 April 2016
Published 31 May 2016

Abstract

Optical rectennas are antenna-coupled diode rectifiers that receive and convert optical-frequency electromagnetic radiation into DC output. The analysis of rectennas is carried out either classically using Maxwell's wave-like approach, or quantum-mechanically using Einstein's particle-like approach for electromagnetic radiation. One of the characteristics of classical operation is that multiple photons transfer their energy to individual electrons, whereas in quantum operation each photon transfers its energy to each electron. We analyze the correspondence between the two approaches by comparing rectenna response first to monochromatic illumination obtained using photon-assisted tunnelling theory and classical theory. Applied to broadband rectenna operation, this correspondence provides clues to designing a rectenna solar cell that has the potential to exceed the 44% quantum-limited conversion efficiency. The comparison of operating regimes shows how optical rectenna operation differs from microwave rectenna operation.

Keywords: rectennas, solar energy, photon-assisted tunneling

(Some figures may appear in colour only in the online journal)

1. Introduction

At radio and microwave frequencies, rectennas are analyzed using classical circuit analysis [1], governed by Maxwell's electromagnetic wave theory. In contrast, the operation of rectennas [2–5] at optical frequencies is fundamentally different from their low frequency response and is described using the theory of photon-assisted tunnelling (PAT) [6, 7], where the quantum interpretation of photon absorption by an electron follows Einstein's particle-like approach to electromagnetic radiation. In figure 1, we illustrate this difference between the classical and quantum regimes, and explain later how this comes about. In the classical case the dark current–voltage [$I(V)$] characteristic is sampled over a range of voltages resulting in a smooth illuminated $I(V)$ response, whereas in the quantum case, the dark $I(V)$ characteristic of the device is sampled at discrete points resulting in a hump in the illuminated $I(V)$. One consequence of the quantum nature of the rectification is to limit the broadband solar conversion efficiency to 44% [8], which is the Trivich–Flinn efficiency limit for quantum processes [9].

Here we apply PAT theory for tunnel junctions [10] to a rectenna equivalent circuit and demonstrate the three different regimes of rectenna operation: classical, quantum, and a transition regime. Although the analysis makes use of tunnel junction $I(V)$ characteristics the conclusions and distinctions between operating regimes are general, and apply to any rectenna operating at the same frequencies and intensities. The requirements for PAT are met by devices where electrons can exchange energy with external alternating fields and their transport between electrodes is phase coherent [11, 12]. These include devices that show quantum effects such as superconductor–insulator–superconductor (SIS) junctions [13], metal–insulator–metal (MIM) diodes [14], resonant tunnelling diodes [15], superlattices [16], quantum dots [17], quantum point contacts [18], small field-effect transistors [19], geometric diodes [20], etc. Of the three components of rectenna operation that could be analyzed quantum mechanically (incident electromagnetic field, current in the antenna, and its rectification) we consider only the rectification process here. We first present the equivalent circuit of the rectenna used in our analysis, and then determine rectenna response

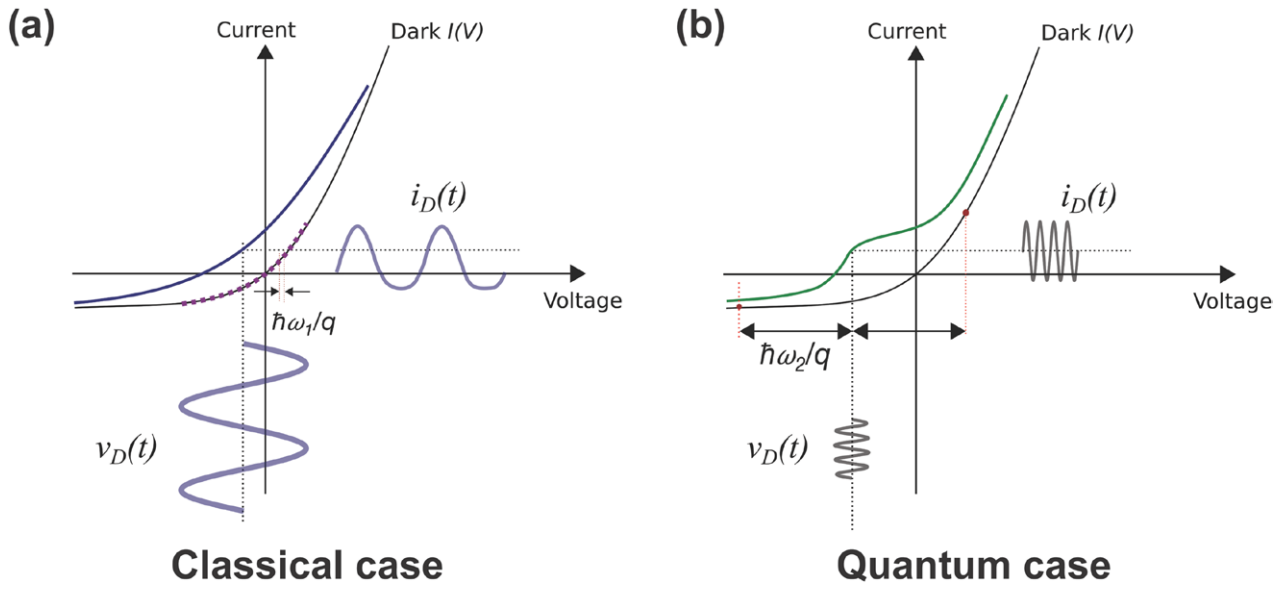

Figure 1. Illustration of the differences between the $I(V)$ characteristics of classical and quantum regimes of rectenna operation. Explanations for these curves are given later in the paper. (a) Dark and illuminated $I(V)$ characteristics of the rectenna in the classical case, which occurs at low frequency (ω_1) and high intensity illumination. The operating point of the rectenna is the intersection of the dotted lines. The dark $I(V)$ is sampled over a continuous range of voltage up to the amplitude of diode voltage [$v_D(t)$] in steps equal to $\hbar\omega_1/q$. (b) Dark (solid black) and illuminated $I(V)$ (solid green) characteristics of the rectenna in the quantum case, which occurs at high frequency (ω_1) and low intensity illumination. The dark $I(V)$ is sampled at discrete voltage steps equal to $\hbar\omega_2/q$. Both classical and quantum cases result in upward shifted illuminated $I(V)$ characteristics.

under different conditions to show the regimes of operation. We apply the results to suggest a rectenna design and setup that has the potential to exceed the 44% conversion efficiency limit by shifting the operation to the classical regime.

2. Rectenna equivalent circuit

To calculate rectenna response and analyze the different regimes of rectenna operation, we use the theory of PAT applied to the rectenna modelled as an equivalent electrical circuit [21]. The equivalent circuit is shown in figure 2, and the procedure to calculate the optical response using PAT is detailed in [7]. In the following, we review the circuit equations for calculating the rectenna response under illumination.

The antenna receives electromagnetic radiation and is represented by a time-dependent source voltage v_S in series with the antenna radiation resistance R_S. The AC input power across the antenna is P_{in}^{AC} and the resulting peak voltage V_S across the antenna under monochromatic illumination is [22]

$$V_S = \sqrt{8R_S P_{in}^{AC}}. \tag{1}$$

A diode connected across the antenna terminals rectifies the AC voltage signal (v_D) to generate AC and DC currents. For most optical rectennas the diode is a metal/insulator/metal (MIM) structure [23–27]. The filter L allows only the rectified DC illuminated current (I_{illum}) to flow to the load R_L giving a DC voltage called the operating voltage V_O, across the diode:

$$|V_O| = I_{illum} R_L. \tag{2}$$

The fact that DC current is blocked from flowing through the antenna is represented in the equivalent circuit by a capacitor

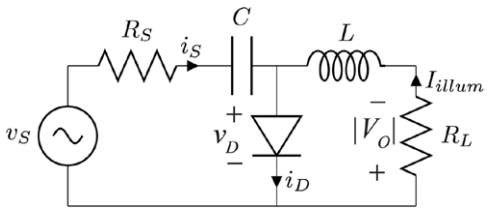

Figure 2. Equivalent circuit of a rectenna. The antenna source voltage is v_S, and its radiation resistance is R_S. The AC current through the antenna circuit is i_S. The total (AC plus DC) voltage across the diode is v_D and the total current through the diode is $i_D = i_S + I_{illum}$. A capacitor C models the blocking of DC current by the antenna, and also provides voltage clamping. The inductor L forms a low-pass filter to block the AC power from being dissipated in the load. The load resistance is R_L and the DC operating voltage across the load is V_O.

C, which clamps the AC input voltage to a DC average of V_O. The net current through the diode (i_D) is the sum of the AC current through the antenna (i_S) and the I_{illum} through the load. The v_D, i_S, and I_{illum} are calculated by applying Kirchhoff's voltage law to the circuit, and iteratively solving the equation

$$v_D(t) = -|V_O| + v_S(t) - i_S(t)R_S. \tag{3}$$

The i_D is calculated using the theory of PAT and the diode dark $I(V)$ characteristics,

$$i_D(t) = \iint d\omega' W(\omega') I_{dark}\left(\omega' + \frac{qV_O}{\hbar}\right) e^{-i\omega' t} d\omega'' W(\omega'') e^{-i\omega'' t}. \tag{4}$$

Angular frequencies ω' and ω'' are integrated from $-\infty$ to $+\infty$. The resulting expression for $i_D(t)$ is a function of those individual frequencies of the incoming wave, their sums and differences, and other combinations. The phase factor W [28]

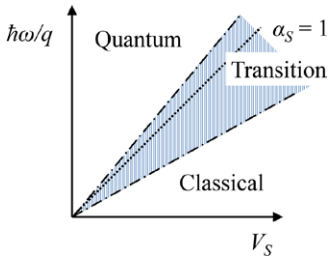

Figure 3. Sketch of the operating regimes of a rectenna as a function of the source voltage ($V_S = \sqrt{8P_{in}R_S}$) and the photon energy divided by the electronic charge ($\hbar\omega/q$). Classical operation occurs when $V_S \gg \hbar\omega/q$, whereas quantum operation occurs when $V_S < \hbar\omega/q$. The ratio of V_S to $\hbar\omega/q$ is α_S, and the hatched blue area around the $\alpha_S = 1$ line (dotted line) is the transition regime.

results from a modulation of the Fermi level in the diode metal contact due to an applied time-dependent perturbation $v_D(t)$, and is related to the diode voltage by the Fourier transform,

$$\int_{-\infty}^{+\infty} d\omega' W(\omega') e^{-i\omega' t} = e^{-i\frac{q}{\hbar}\int^{t} dt'[v_D(t')]}. \quad (5)$$

Additional information about the terms in equations (4) and (5), and examples calculating the diode current under illumination are given in [6, 29]. The DC output power P_{out}^{DC} and the efficiency η are given by,

$$P_{out}^{DC} = |V_O| I_{illum}. \quad (6)$$

$$\eta = \frac{P_{out}^{DC}}{P_{in}^{AC}}. \quad (7)$$

In our calculations, we first determine the $v_S(t)$ from the input conditions, and use equations (3)–(5) iteratively to calculate $i_D(t)$, $i_S(t)$, and $v_D(t)$ at discrete V_O. Using $i_D(t)$ we calculate the I_{illum} and η for different V_O, then plot the V_O versus I_{illum} and η results.

3. Operating regimes of the rectenna

We show that the rectenna operates in one of the three regimes based on the amplitude of the diode AC voltage (V_D) relative to the photon energy divided by the electronic charge ($\hbar\omega/q$), with this ratio denoted by the parameter α,

$$\alpha = \frac{qV_D}{\hbar\omega}. \quad (8)$$

Since V_D is a dynamic quantity and changes with V_O, for simplicity we will use V_S as an approximation for V_D to determine the operating regime. For a piecewise linear diode used here, V_D can vary from $V_S/2$ to V_S depending on the diode forward resistance and V_O, and therefore α_S is a good approximation for α. The three regimes, sketched in figure 3, are

a. Quantum regime: $\alpha_S < 1$
b. Transition regime: $\alpha_S \sim 1$
c. Classical regime: $\alpha_S \gg 1$

In the following, we analyze rectenna operation under monochromatic illumination in each of the three regimes, with the goal of understanding the characteristics in each regime. To make the differences easily discernable, we use the following assumptions in our calculations: the diode dark $I(V)$ characteristics (I_{dark}) may be approximated with a piecewise linear curve with zero reverse leakage current and a forward resistance (R_f) of 50 Ω such that its secant resistance [6] (described in section 3.1, below) at $V_O = 0$ is 100 Ω, R_S is 100 Ω to roughly match the impedance of free-space, the diode capacitance is negligible so that the rectification is not RC-time-constant limited, the diode is at 0 K and does not produce thermal noise, and the antenna efficiency [30] is unity. A simple rule of thumb to estimate the analysis regime is as follows: classical analysis is sufficient at 1 THz for tens of millivolts of input voltage, which would correspond to solar intensity (100 mW cm^{-2}) absorbed over an area of ~100 μm^2 (0.1 μW). PAT analysis is required for the same power and voltage at ~30 THz and above. Unless noted otherwise, all calculations that follow were performed using PAT theory following the method outlined in section 2.

3.1. Quantum regime ($\alpha_S < 1$)

The rectenna operates in the quantum regime when $\hbar\omega/q > V_S$ according to PAT theory, and electrons can absorb only individual photons. A sinusoidal time-dependent voltage applied across the rectenna diode affects the phase of the electrons on one electrode relative to the other, and results in an electron wave function having discrete energy states separated by the photon energy of the incoming field (see [6] for a mathematical description). Each state is weighted by a Bessel term that is a function of the amplitude and frequency of the applied voltage. As a result, the I_{illum} is quantized and results in discrete steps in the illuminated $I(V)$ characteristics. We can simplify and average the expression in (4) to express I_{illum} as

$$I_{illum} = \sum_{n=-\infty}^{\infty} J_n^2\left(\frac{qV_D}{\hbar\omega}\right) . I_{dark}\left(V_O + n\frac{\hbar\omega}{q}\right). \quad (9)$$

Here n is the number of photons absorbed or emitted by an electron in the diode. For small $qV_D/\hbar\omega$, the Bessel terms in (9) are significant only for $n = -1$, 0, and 1. Therefore, the I_{illum} depends on I_{dark} at discrete voltages $\hbar\omega/q$ above and below the V_O (which is also the reason that the previously mentioned secant resistance [6] is a function of the secant between two points on the $I(V)$). The resulting diode current responsivity is,

$$\beta = \frac{q}{\hbar\omega}\left[\frac{I_{dark}\left(V_O + \frac{\hbar\omega}{q}\right) - 2I_{dark}(V_O) + I_{dark}\left(V_O - \frac{\hbar\omega}{q}\right)}{I_{dark}\left(V_O + \frac{\hbar\omega}{q}\right) - I_{dark}\left(V_O - \frac{\hbar\omega}{q}\right)}\right]. \quad (10)$$

For asymmetric tunnel diodes where $[I_{dark}(V_O + \hbar\omega/q) - I_{dark}(V_O) \gg I_{dark}(V_O) - I_{dark}(V_O - \hbar\omega/q)]$, the diode current responsivity approaches $q/\hbar\omega$ [28], which means that for each incoming photon at most one electron tunnels through the barrier. A high-speed and sufficiently asymmetric diode can detect single photons in weak optical signals, but for $V_O \leqslant -\hbar\omega/q$ the rectified current drops to zero, as is evident in the following two sets of figures.

Using the method outlined in the previous section, we calculate the response of the diode in a rectenna under different input conditions to demonstrate its operation in the quantum regime. The three cases correspond to small α ($\alpha_S \sim 0.1$, 0.05, and 0.03) and different incident frequencies (0.1 eV, 0.2 eV, and 1 meV). With change in frequency, the P_{in} has to be adjusted in each case so that the rectenna is in the quantum regime. We choose two different frequencies to show that the response is frequency dependent (shown in figures 4(a) and (b) for 0.1 eV and 0.2 eV), and quantum operation of the rectenna is not limited to infrared (IR) and optical frequencies, but also applies at microwave frequencies (shown in figure 4(c) for 1 meV) for very low input powers. Since $\alpha_S < 1$, the rectenna operates in the quantum regime and the results follow the qualitative argument presented above, i.e. electrons absorb photons when $|V_O| < \hbar\omega/q$ to generate a photocurrent which decreases to zero as $|V_O| \leqslant \hbar\omega/q$. As a result, in the quantum regime current is produced only when V_O is within $\hbar\omega/q$ of the origin, and therefore photons cannot be used to generate current at voltages greater than $\hbar\omega/q$.

3.2. Transition regime ($\alpha_S \sim 1$)

As the V_S exceeds $\hbar\omega/q$, electrons absorb multiple photons and the rectenna operates in the transition regime. Here the discrete nature of the illuminated $I(V)$ is maintained, but starts approaching the classical response. The discrete behaviour is seen in the form of steps in the illuminated $I(V)$ that occur at integer multiples of $\hbar\omega/q$. In figure 5, we plot the rectenna response for $\alpha_S \sim 2.8$ and $\hbar\omega = 0.1$ eV. As $|V_O| > 0.1$ V, electrons that absorb single photons have insufficient energy to generate a photocurrent, and the contribution of these electrons (called the first-order photon absorption term, corresponding to $n = 1$ in (9)) to I_{illum} reduces to zero. The second-order absorption (electrons absorbing two photons) continues to contribute to the I_{illum} up to $V_O = -0.2$ V, which results in a second step in the illuminated $I(V)$. As the $|V_O|$ is increased, the successive higher order absorptions give a step-like behaviour. The shapes of efficiency plots in these figures exhibit the characteristics of each regime. Their magnitudes depend upon the particular illumination intensities and diode parameters and are not by themselves significant.

3.3. Classical regime ($\alpha_S \gg 1$)

When $V_S \gg \hbar\omega/q$ each electron absorbs many photons. Electron excitations occur at multiple energies, such that the PAT response of the diode to illumination is essentially equal to the classical response. Mathematically, applying the limit of large α_S and converting the summation of equation (9) into an integral form, the expression for I_{illum} in (9) reduces to the classical case (see [31] for detailed mathematics),

$$I_{illum} = \frac{1}{\pi}\int_{-\pi/2}^{\pi/2} I_{dark}(V_O + V_D \sin\theta)\mathrm{d}\theta. \qquad (11)$$

All calculations for the classical regime were done using PAT theory, and so $\hbar$ appears in the calculations. When the theory is taken to the classical limit, $\hbar$ vanishes in the final result,

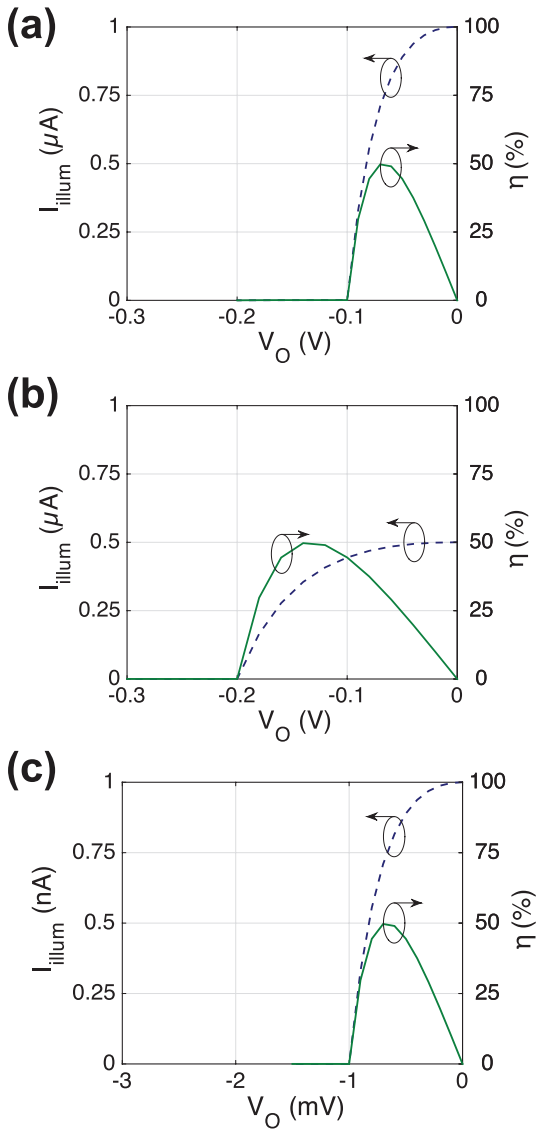

Figure 4. Quantum regime $I(V)$ (dashed blue) and efficiency (solid green) characteristics of a rectenna under monochromatic illumination, to show the response of the rectenna at infrared (IR) frequencies, and at microwave frequencies for low input power. The diode $I(V)$ characteristics are piecewise linear with a forward resistance of 50 Ω and zero reverse leakage. Quantum operation of the rectenna at (a) Incident photon energy $\hbar\omega = 0.1$ eV for small $\alpha_S \sim 0.1$ ($P_{in} = 100$ nW), (b) $\hbar\omega = 0.2$ eV for small $\alpha_S \sim 0.05$, ($P_{in} = 100$ nW). (c) $\hbar\omega = 1$ meV for small $\alpha_S \sim 0.03$ ($P_{in} = 1$ pW) showing quantum operation of the rectenna at microwave frequencies for very low input powers. Unlike classical theory where the response is independent of frequency, the I_{illum} is frequency dependent and is non-zero for $|V_O| < \hbar\omega/q$.

as it does in equation (11). Shown in figure 6(a) is the rectenna response at microwave frequencies ($\hbar\omega = 1$ meV), as in figure 4(c), but at a higher P_{in} of 1 μW, which results in classical operation. As we will see for the case of broadband illumination, classical operation provides significant advantages for conversion efficiency if it can be attained at higher frequencies. The classical response can occur at optical and IR wavelengths, but requires large V_D, which can be achieved in two ways: increasing the input power, and increasing the source and diode impedances.

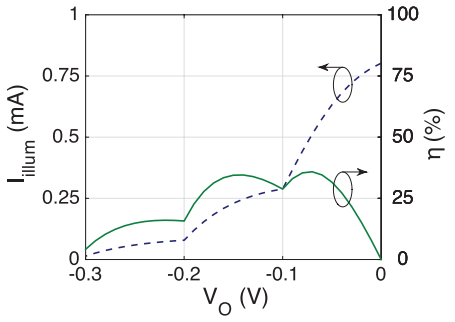

Figure 5. Transition regime $I(V)$ (dashed blue) and efficiency (solid green) characteristics of a rectenna operating under monochromatic illumination for the diode of figure 4, showing discrete steps at integer multiples of $\hbar\omega/q$. The $\hbar\omega$ is 0.1 eV and the P_{in} is 100 μW, giving $\alpha_S = 2.8$. The steps in the I_{illum} at $V_O = -0.1$ V and $V_O = -0.2$ V are due to the second and third-order photon absorptions resulting in a non-zero current for $V_O < -0.1$ V and $V_O < -0.2$ V.

a. *Increasing the input power:* A large voltage across the antenna results in a large voltage across the matched diode. In figure 6(b), we plot the illuminated $I(V)$ characteristics of the rectenna for $P_{in} = 10$ mW, and $\hbar\omega = 0.1$ eV, resulting in $\alpha_S = 28$. The PAT and classical results are virtually identical to each other.

b. *Increasing the source impedance*: Increasing the R_S results in a larger V_S for the same input intensity, according to (1), but a large R_S requires a high impedance diode for good impedance match. An $R_S = 1$ MΩ, $R_f = 500$ kΩ, $P_{in} = 1$ μW, and $\hbar\omega = 0.1$ eV results in the same α_S as in (a), above, and the illuminated $I(V)$ characteristic of the rectenna approaches the classical result, as shown in figure 6(c) (in reality, such large resistances would result in far too large an RC time constant for optical frequency rectification, but may be acceptable for microwave rectennas).

In the three cases shown in figure 6, I_{illum} is a smooth function of the V_O and decreases to zero as the V_O exceeds the amplitude of the v_D. The discrete steps in the I_{illum} that were evident for the quantum case are not noticeable even as the frequency approaches 30 THz.

The maximum efficiency of the rectenna under monochromatic illumination in the classical case is lower than the efficiency in quantum regime because of the additional power loss in the higher order harmonic currents generated due to multiphoton absorption, as in the transition regime. However, the classical regime can have a positive effect on the efficiency of harvesting broadband radiation because low energy photons of different frequencies mix and excite electrons to higher energy levels, and used at higher operating voltages. The absence of such mixing in the quantum rectification of low intensity broadband solar radiation limits the maximum efficiency to 44%, as was shown in [8].

4. Application to broadband rectification

To demonstrate that broadband rectenna operation in the classical regime results in a higher efficiency of rectification

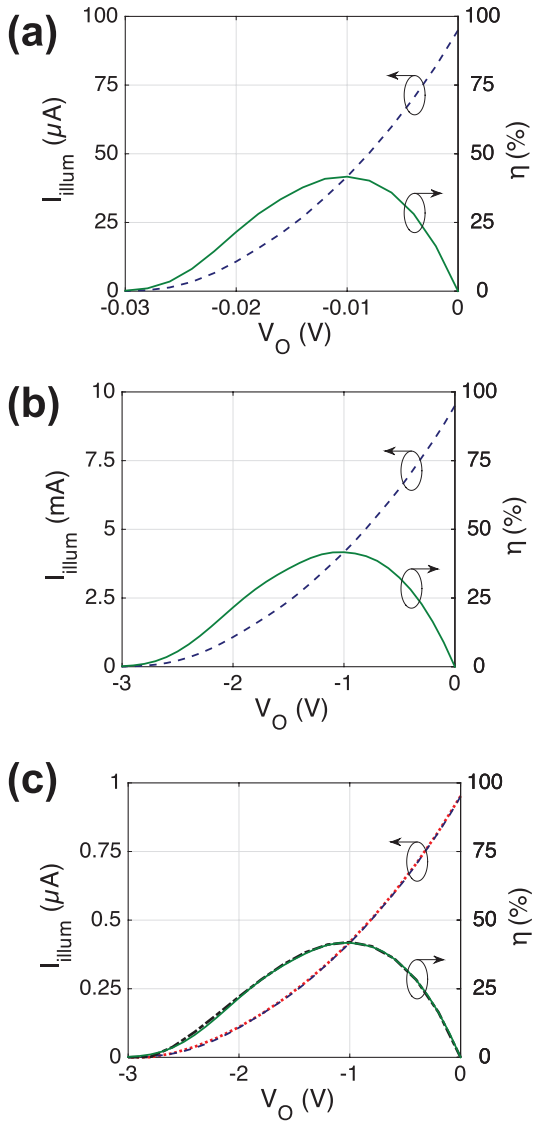

Figure 6. Classical regime $I(V)$ (dashed blue) and efficiency (solid green) of a rectenna operating under monochromatic illumination, calculated using PAT theory under different input conditions, such that the $V_S \gg \hbar\omega/q$. The diode has piecewise linear $I(V)$ with zero reverse leakage. (a) As expected at microwave frequencies, when the P_{in} is high so that V_S and $V_D \gg \hbar\omega/q$ (1 μW with $R_f = 50$ Ω and $\hbar\omega = 1$ meV), the response is classical. To demonstrate the two ways to achieve large V_S compared to $\hbar\omega/q$ resulting in classical operation at IR frequencies ($\hbar\omega = 0.1$ eV), using (b) large $P_{in} = 10$ mW (with $R_f = 50$ Ω, $R_S = 100$ Ω), and (c) large $R_S = 1$ MΩ ($R_f = 500$ kΩ, and $P_{in} = 1$ μW). Also plotted are the illuminated $I(V)$ (dotted red) and efficiency (dash-dot black) characteristics calculated using classical theory that superimpose with the PAT theory results, showing that the classical theory and PAT theory results are identical in the classical regime. Although not shown, the same applies to results in (a) and (b).

compared to the quantum regime, we calculate the rectenna response to blackbody illumination under different operating conditions. In our calculations, we choose the temperature of the blackbody and two different conditions such that the rectenna operates in classical and in quantum regimes. We confirm classical rectenna operation under high V_S by comparing the PAT response with the response calculated using classical

theory. Then we compare the ultimate efficiency of the rectenna in the quantum regime with its efficiency in the classical regime for varying diode resistances and show that the classical regime can be more efficient.

We use a 3D blackbody spectrum of temperature 600 K. We choose 600 K because for values of P_{in} and R_S used here ($P_{in} = 100$ μW, $R_S = 10$ KΩ), the resulting V_S (rms) is high relative to the $\hbar\omega/q$ at which the peak in the blackbody spectrum occurs (~0.15 eV), and therefore the rectenna operates in the classical regime. Comparing results calculated from PAT theory to the I_{illum} and η calculated using classical theory shows that the two results superimpose each other, as in figure 7(a), confirming that the input conditions are appropriate for classical operation of the rectenna.

The quantum regime occurs when the P_{in} and R_S are such that the V_S (rms) is low compared to the peak $\hbar\omega/q$ of the blackbody spectrum, and is shown in figure 7(b) (for $P_{in} = 100$ nW, $R_S = 100$ Ω). The resulting range of V_O over which rectenna operates is smaller than in the classical regime, and the electrons are used at $V_O \sim \hbar\omega/q$ to generate current. Therefore, the efficiency of quantum operation is expected to be lower than classical operation. The peak efficiency (η_{peak}) is 37.5% and is lower than the classical η_{peak} of 41%.

The low efficiency in the broadband quantum regime could be due to a poor impedance match between the antenna and the diode. To remove the effect of impedance matching, we calculate the ultimate rectenna efficiency for an ideal diode that is matched with the antenna at every V_O [8]. We found the maximum efficiency in this quantum regime case to be ~44% for solar radiation, and the maximum efficiency number is the same for radiation from a blackbody of any temperature. We compare this ultimate efficiency with the classical η_{peak} versus the R_f, calculated using classical theory, showing in figure 7(c) that the operation of broadband rectennas in the classical regime can exceed the quantum-limited efficiency. The η_{peak} decreases with increasing R_f due to decreasing impedance match with the antenna, but is greater at small R_f than the ultimate efficiency in the quantum regime.

Despite the improvement in the theoretical efficiency for classical operation of the rectenna compared to quantum operation, there are practical challenges of operating the rectenna in the regimes of figures 7(a) and (c), especially for sources with low intensity and high frequency radiation such as the sun. A drawback of increasing the R_S is an increase in the rectenna RC time constant and a decrease in the coupling efficiency [27, 32]. In addition, increasing the radiation resistance of the antenna is an engineering challenge. However, designs such as the traveling-wave diode [25, 33], geometric diode [34], carbon nanotube forests [35], and the sharp tip configurations [36] mitigate the effect of the RC time constant and can potentially be used together with this technique.

A second problem that limits the increase in V_S is the diode breakdown voltage. MIM diodes, used in rectennas for high frequency rectification, work on the principle of electron tunnelling through nanometre-scale thin oxides [37–41]. The breakdown strength of oxides is of the order of 1 MV cm^{-1} [42], resulting in a breakdown voltage of 1 V across a 10 nm thick tunnelling layer. This makes harvesting of high frequency solar radiation difficult, because classical operation requires $V_S \gg \hbar\omega/q$.

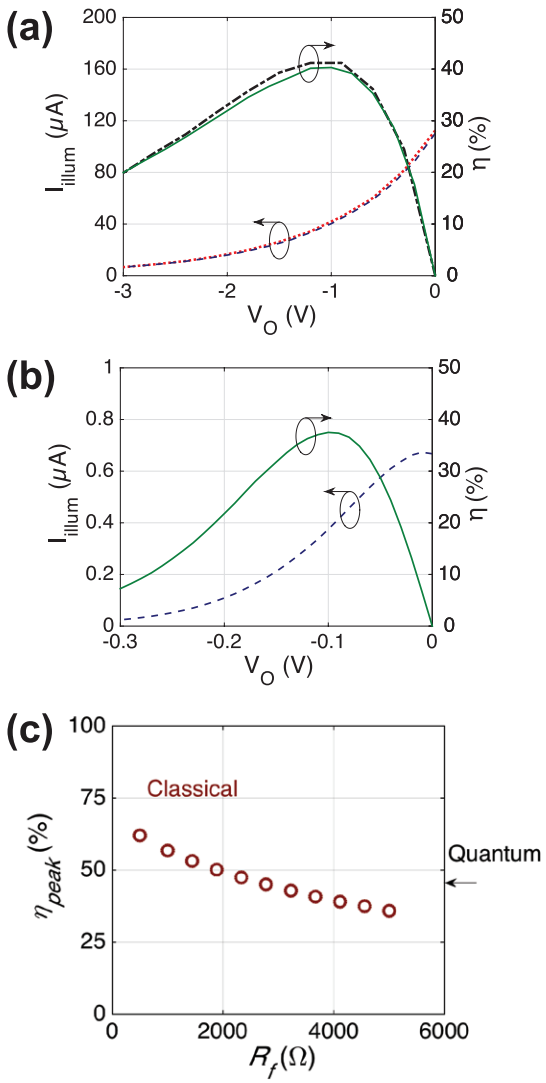

Figure 7. Comparison of classical and quantum operation for rectennas under broadband illumination from a blackbody of temperature 600 K, showing $I(V)$ (dashed blue) and efficiency (solid green) characteristics. The diode is a piecewise linear diode with zero reverse leakage current. (a) Classical operation of the rectenna occurs at large P_{in} and R_S (when $P_{in} = 100$ μW, $R_f = 3$ kΩ, and $R_S = 10$ kΩ) giving high V_S (rms) compared to the $\hbar\omega/q$ at which the blackbody spectrum peaks, and the results closely superimpose over the classical theory results (dotted red and dash-dot black). The peak efficiency (η_{peak}) is 41%. (b) Quantum operation of the rectenna occurs at small $P_{in} = 100$ nW and $R_S = 100$ Ω ($R_f = 30$ Ω). The rectenna operates efficiently over a smaller range of V_O compared to the classical case and the resulting peak efficiency is lower at 37.5%. (c) Variation of the peak efficiency (η_{peak}) of the rectenna (red circles), calculated using classical theory, with change in the diode R_f. Broadband classical operation is more efficient than quantum operation of the rectenna where the ultimate efficiency is 44%.

The third problem is the limited spatial coherence of radiation from blackbody sources [43, 44]. Since input intensities are low and the radiation from blackbodies is coherent only over small areas, the rectenna must be small and receives only

enough optical power to operate in the quantum regime, such that the resulting efficiency of energy harvesting is limited.

For these three reasons achieving classical operation of rectennas for energy harvesting of high temperature blackbody radiation is a challenge, and new solutions are required for rectennas to exceed the Trivich–Flinn efficiency limit [9]. New rectenna designs such as those based on carbon nanotube forests could alleviate some of these issues [35, 45].

5. Summary

If broadband rectennas operate in the quantum regime, their efficiency is limited to the maximum efficiency for quantum conversion [8] that also limits conventional solar cells, which is 44% for the solar spectrum. Conventional rectifiers are not subject to this limit because they usually operate in the classical regime. Therefore, shifting from the quantum to the classical regime of operation for optical rectennas provides the potential for substantially higher conversion efficiencies. We investigated rectenna operation using the quantum theory of photon-assisted tunnelling under different operating conditions. We found that there are different regimes of rectenna operation, from quantum to classical. Rectennas follow Einstein's photon-based approach if the diode voltage (V_S) is less than the photon energy divided by the electronic charge ($\hbar\omega/q$), and follow Maxwell's classical electromagnetic wave nature of light if $V_S \gg \hbar\omega/q$. The correspondence between classical and quantum operation of the rectenna in the limit of large V_S compared to $\hbar\omega/q$ allows classical operation at optical and IR frequencies for high incident intensity and for large source and diode impedances.

Additional information

Competing financial interests: GM holds stock in RedWave Energy, Inc.

Acknowledgments

This work was carried out under contracts from Abengoa Solar and RedWave Energy Inc. For some of the results presented here we used the Janus supercomputer, which is supported by the National Science Foundation (award number CNS-0821794), the University of Colorado Boulder, the University of Colorado Denver, and the National Center for Atmospheric Research. The Janus supercomputer is operated by the University of Colorado Boulder. The authors thank Amina Belkadi, Bradley Pelz, and Shuai Yuan for helpful suggestions to improve the manuscript.

References

[1] McSpadden J O, Fan L and Chang K 1998 Design and experiments of a high-conversion-efficiency 5.8 GHz rectenna *IEEE Trans. Microw. Theory Tech.* **46** 2053–60
[2] Sarehraz M, Buckle K, Weller T, Stefanakos E, Bhansali S, Goswami Y and Krishnan S 2005 Rectenna developments for solar energy collection *Conf. Record of the 31st IEEE Photovoltaic Specialists Conf. 2005* pp 78–81
[3] Bean J A, Weeks A and Boreman G D 2011 Performance optimization of antenna-coupled tunnel diode infrared detectors *IEEE J. Quantum Electron.* **47** 126–35
[4] Moddel G 2013 Will rectenna solar cells be practical? *Rectenna Solar Cells* ed G Moddel and S Grover (Berlin: Springer) pp 3–24
[5] Yu F, Moddel G and Corkish R 2014 Quantum rectennas for photovoltaics *Advanced Concepts in Photovoltaics* ed A J Nozik *et al* (Cambridge: Royal Society of Chemistry) pp 506–46
[6] Grover S, Joshi S and Moddel G 2013 Quantum theory of operation for rectenna solar cells *J. Phys. D: Appl. Phys.* **46** 135106
[7] Haus J W, de Ceglia D, Vincenti M A and Scalora M 2014 Quantum conductivity for metal-insulator-metal nanostructures *J. Opt. Soc. Am.* B **31** 259
[8] Joshi S and Moddel G 2013 Efficiency limits of rectenna solar cells: theory of broadband photon-assisted tunneling *Appl. Phys. Lett.* **102** 083901
[9] Trivich D and Flinn P A 1955 Maximum efficiency of solar energy conversion by quantum processes *Solar Energy Research* ed F Daniels and J A Duffie (Madison, WI: University of Wisconsin Press)
[10] Mead C A 1961 Operation of tunnel-emission devices *J. Appl. Phys.* **32** 646–52
[11] Jauho A-P, Wingreen N S and Meir Y 1994 Time-dependent transport in interacting and non-interacting mesoscopic systems *Phys. Rev.* B **50** 5528–44
[12] Kouwenhoven L P, Jauhar S, Orenstein J, McEuen P L, Nagamune Y, Motohisa J and Sakaki H 1994 Observation of photon-assisted tunneling through a quantum dot *Phys. Rev. Lett.* **73** 3443–6
[13] Dayem A H and Martin R J 1962 Quantum interaction of microwave radiation with tunneling between superconductors *Phys. Rev. Lett.* **8** 246–8
[14] Marshalek R and Davidson F M 1983 Photoresponse characteristics of thin-film nickel–nickel oxide–nickel tunneling junctions *IEEE J. Quantum Electron.* **19** 743–54
[15] Drexler H, Scott J S, Allen S J, Campman K L and Gossard A C 1995 Photon-assisted tunneling in a resonant tunneling diode: stimulated emission and absorption in the THz range *Appl. Phys. Lett.* **67** 2816–8
[16] Keay B J, Allen S J, Galán J, Kaminski J P, Campman K L, Gossard A C, Bhattacharya U and Rodwell M J W 1995 Photon-assisted electric field domains and multiphoton-assisted tunneling in semiconductor superlattices *Phys. Rev. Lett.* **75** 4098–101
[17] Kouwenhoven L P, Jauhar S, McCormick K, Dixon D, McEuen P L, Nazarov Y V, van der Vaart N C and Foxon C T 1994 Photon-assisted tunneling through a quantum dot *Phys. Rev.* B **50** 2019–22
[18] Hu Q 1993 Photon-assisted quantum transport in quantum point contacts *Appl. Phys. Lett.* **62** 837–9
[19] Bykov A, Gusev Z, Kvon Z and Fomin B 1990 Fluctuation properties of small silicon field-eff ect transistors *Pis'ma Zh. Eksp. Teor. Fiz.* **97** 1–262
[20] Grover S and Moddel G 2013 Optical frequency rectification *Rectenna Solar Cells* ed G Moddel and S Grover (Berlin: Springer) pp 25–46
[21] Joshi S and Moddel G 2015 Rectennas at optical frequencies: how to analyze the response *J. Appl. Phys.* **118** 084503
[22] Orfanidis S J 2002 *Electromagnetic Waves and Antennas* (New Brunswick, NJ: Rutgers University)
[23] Faris S, Gustafson T and Wiesner J 1973 Detection of optical and infrared radiation with DC-biased electron-tunneling metal-barrier-metal diodes *IEEE J. Quantum Electron.* **9** 737–45

[24] Heiblum M, Wang S, Whinnery J R and Gustafson T 1978 Characteristics of integrated MOM junctions at DC and at optical frequencies *IEEE J. Quantum Electron.* **14** 159–69
[25] Hobbs P C D, Laibowitz R B, Libsch F R, LaBianca N C and Chiniwalla P P 2007 Efficient waveguide-integrated tunnel junction detectors at 1.6 μm *Opt. Express* **15** 16376–89
[26] Krishnan S, Stefanakos E and Bhansali S 2008 Effects of dielectric thickness and contact area on current–voltage characteristics of thin film metal-insulator-metal diodes *Thin Solid Films* **516** 2244–50
[27] Grover S and Moddel G 2011 Applicability of metal/insulator/metal (MIM) diodes to solar rectennas *IEEE J. Photovolt.* **1** 78–83
[28] Tucker J R 1979 Quantum limited detection in tunnel junction mixers *IEEE J. Quantum Electron.* **15** 1234–58
[29] Joshi S, Grover S and Moddel G 2013 Efficiency limits for solar spectrum rectification *Rectenna Solar Cells* ed G Moddel and S Grover (Berlin: Springer) pp 47–67
[30] Ma Z and Vandenbosch G A E 2013 Optimal solar energy harvesting efficiency of nano-rectenna systems *Sol. Energy* **88** 163–74
[31] Hamilton C A and Shapiro S 1970 RF-induced effects in superconducting tunnel junctions *Phys. Rev.* B **2** 4494–503
[32] Sanchez A, Davis C F, Liu K C and Javan A 1978 The MOM tunneling diode: theoretical estimate of its performance at microwave and infrared frequencies *J. Appl. Phys.* **49** 5270–7
[33] Grover S, Dmitriyeva O, Estes M J and Moddel G 2010 Traveling-wave metal/insulator/metal diodes for improved infrared bandwidth and efficiency of antenna-coupled rectifiers *IEEE Trans. Nanotechnol.* **9** 716–22
[34] Zhu Z, Joshi S, Grover S and Moddel G 2013 Graphene geometric diodes for terahertz rectennas *J. Phys. D: Appl. Phys.* **46** 185101
[35] Sharma A, Singh V, Bougher T L and Cola B A 2015 A carbon nanotube optical rectenna *Nat. Nanotechnol.* **10** 1027–32
[36] Miskovsky N M, Cutler P H, Mayer A, Weiss B L, Willis B, Sullivan T E and Lerner P B 2012 Nanoscale devices for rectification of high frequency radiation from the infrared through the visible: a new approach *J. Nanotechnol.* **2012** 1–19
[37] Choi K, Yesilkoy F, Ryu G, Cho S H, Goldsman N, Dagenais M and Peckerar M 2011 A focused asymmetric metal-insulator-metal tunneling diode: fabrication, DC characteristics and RF rectification analysis *IEEE Trans. Electron Devices* **58** 3519–28
[38] Periasamy P, Berry J J, Dameron A A, Bergeson J D, Ginley D S, O'Hayre R P and Parilla P A 2011 Fabrication and characterization of MIM diodes based on Nb/Nb_2O_5 via a rapid screening technique *Adv. Mater.* **23** 3080–5
[39] Cowell E W, Alimardani N, Knutson C C, Conley J F, Keszler D A, Gibbons B J and Wager J F 2011 Advancing MIM electronics: amorphous metal electrodes *Adv. Mater.* **23** 74–8
[40] Grover S and Moddel G 2012 Engineering the current–voltage characteristics of metal-insulator-metal diodes using double-insulator tunnel barriers *Solid-State Electron.* **67** 94–9
[41] Alimardani N and Conley J F 2013 Step tunneling enhanced asymmetry in asymmetric electrode metal-insulator–insulator-metal tunnel diodes *Appl. Phys. Lett.* **102** 143501
[42] McPherson J W, Kim J, Shanware A, Mogul H and Rodriguez J 2003 Trends in the ultimate breakdown strength of high dielectric-constant materials *IEEE Trans. Electron Devices* **50** 1771–8
[43] Mashaal H and Gordon J M 2011 Fundamental bounds for antenna harvesting of sunlight *Opt. Lett.* **36** 900–2
[44] Mashaal H and Gordon J M 2013 Solar and thermal aperture antenna coherence performance limits *Rectenna Solar Cells* ed G Moddel and S Grover (Berlin: Springer) pp 69–86
[45] Moddel G 2015 Optical rectennas: nanotubes circumvent trade-offs *Nat. Nanotechnol.* **10** 1009–10